International Journal of Technology 15(5) 1502-1523 (2024)
Received April 2024 / Revised May 2024 / Accepted June 2024

International Journal of Technology

http://ijtech.eng.ui.ac.id

Comparison Between Cubic and Quadratic Models of Hydrodynamic Derivatives to the Ship Course Stability Index

Fakhri Akbar Ayub[1*], Yoshitaka Furukawa[2]

[1]*Naval Architecture and Marine Engineering, Faculty of Engineering, Universitas Pembangunan Nasional "Veteran" Jakarta, 12450, Jakarta, Indonesia*
[2]*Department of Marine Systems Engineering, Faculty of Engineering, Kyushu University, Fukuoka 819-0395, Japan*

Abstract. The mathematical equations that describe the hydrodynamic forces on a ship's hull are important in understanding how a ship moves. These equations are based on specific values that vary depending on the type of ship. This research will focus on a mathematical model based on a polynomial model in order to investigate the differences between the 3rd order polynomial (cubic model) and the 2nd order polynomial (quadratic model). The course stability index is determined by utilizing linear hydrodynamic derivatives and examined to understand the distinctions between the characteristics of cubic and quadratic models. In this research, the measurement data of the hydrodynamic forces of 12 model vessels (total of 27 loading conditions) that had been conducted for turning tests and the zigzag tests in the past at Kyushu University were targeted. The $\boldsymbol{\beta}$ based 2nd order model and the $\boldsymbol{v'}$ based 3rd order model are applied for re-analysis, and the results of a comparative study on the difference and approximation characteristics of the hydrodynamic force due to the difference of the adopted models are shown.

Keywords: Course stability index; Cubic model; hydrodynamic derivatives; Ship manoeuvrability; Quadratic model

1. Introduction

The International Maritime Organization (IMO) has approved Resolution A.751(18), known as the Interim Standards for Ship Manoeuvrability, in order to improve marine safety by removing ships with inadequate manoeuvrability. Currently, the issue of manoeuvring subjects has become significant due to the establishment of criteria for manoeuvring characteristics in the Standards for Ship Manoeuvrability Criteria (IMO, 2002). The IMO has identified ship manoeuvrability as a critical factor in a ship's ability to change or maintain its course and speed. Larger ships, in particular, often encounter greater challenges in navigation due to their limited manoeuvrability. Any ship that is exceeds 100 meters in length must meet the requirements outlined in the IMO's manoeuvring standards.

Manoeuvring performance of a ship should be evaluated properly at the design phase in order to eliminate ships that, have poor manoeuvrability. Several methods to evaluate at the design stage have been developed such as direct and indirect methods (Hasanvand and Hajivand, 2019). Numerical simulations based on a mathematical model of hydrodynamic

*Corresponding author's email: fakhriakbar@upnvj.ac.id, Tel.: +62811942313
doi: 10.14716/ijtech.v15i5.7036

forces acting on a ship is one of the evaluation methods for indirect methods.

Moreover, the manoeuvring standards require to prove that a newly constructed ship meets the requirements for manoeuvring tests under fully loaded conditions in calm weather. During this process, numerical simulation plays a key role in ensuring the accuracy of hydrodynamic coefficients in mathematical models that depict the forces affecting a ship's manoeuvring abilities.

The hydrodynamic forces on a ship's hull are mathematically represented by specific values known as hydrodynamic derivatives. These derivatives vary depending on the type of ship and are determined by analyzing the measured forces acting on the hull. They indicate the rate of change of the forces and moments. Hydrodynamic derivatives can also be expressed as a function of a ship's principal particulars, including length, beam, draught, trim, and displacement (Kijima *et al.,* 1990).

Additionally, there are various types of errors and uncertainties present in mathematical models of hydrodynamic forces that are utilized in predicting manoeuvring motions. (Dash, Nagarajan, and Sha, 2015; Wang *et al.,* 2014). These issues are often related to the hydrodynamic derivatives that represent the hydrodynamic forces acting on a ship hull. (Ayub, Furukawa, and Ibaragi, 2021; Shenoi, Krishnankutty, and Selvam, 2015), model tests (Woodward, 2013), facilities equipment (Gavrilin and Steen, 2016; Woodward, 2014). Extrapolation of data may occur when applying the results of a mathematical model to drift angles and rotation rates that have not been tested within the model's range (ITTC Manoeuvring Committee, 2017; 2008).

Analyzing and evaluating errors can be a challenging and time-intensive process, but it's necessary for validation. The accuracy of predicted results relies on the methods used to predict manoeuvring performance. Therefore, it is essential to make a dedicated effort to verify and validate prediction or simulation methods in order to accurately assess their accuracy. In order to properly evaluate the correlation between predicted outcomes and actual hydrodynamic forces, it is important to consider uncertainties in both the predictions and the measured data.

A brief review of the mathematical models has been summarized by the International Towing Tank Conference (ITTC Manoeuvring Committee, 2011). Each method has it own advantages and disadvantages. The mathematical model for manoeuvring motions is categorized into several models such as; cross-flow model (Yoshimura, 1988; Oltmann and Sharma, 1984), Polynomial model (Viallon, Sutulo, and Soares, 2012), Manoeuvring Modelling Group Model (Yasukawa and Yoshimura, 2015), Fourier expansion model (Toxopeus, 2011a; 2011b; 2007; Kang and Hasegawa, 2007), Karasuno's model (Karasuno *et al*., 2003), Vectorial model (Berge and Fossen., 2012; Fossen, 2011), RANS CFD (Liu *et al*, 2021; Islam and Soares, 2018).

The basic principles of the equations of motion for ship manoeuvring are based on Newton's second law of motion (Tao *et al*, 2021). The first theoretical approach focused on analyzing the ship as a rigid body with movements in surge, sway, and yaw and explaining the hydrodynamic forces and moments on the ship through first-order derivatives.

Nonlinear hydrodynamic forces were found to be present at high velocities and when cross products of velocities occurred, causing forces and moments to deviate from linear behaviour. These non-linear forces can become comparable in magnitude to the linear component during a sharp turn with a significant rudder angle. Moreover, the yawing moment's non-linear aspect is typically five to ten times greater than its linear component. These non-linear terms are often depicted using cubic or quadratic polynomial equations, with coefficients typically established through captive model tests.

The Taylor series expansion is employed to represent the non-linearities, leading to a polynomial expression involving two variables (Luo *et al*., 2016). The hydrodynamic forces and moments acting on a ship can result in a variety of motions and orientation parameters. By utilizing the Taylor series expansion of a function with multiple variables, these functions can be simplified into a more manageable mathematical form. In this scenario, the sway forces and yawing moment can be accurately represented by using only the odd terms in the Taylor series due to the symmetry between port and starboard.

Alternatively, the non-linearities could be accounted for using quadratic polynomial expressions (Fedyaevsky and Sobolev, 1963a). Although second-order terms may not be ideal since they are even functions, this issue can be circumvented by incorporating a modulus term and adjusting the way the non-linearities are expressed. The quadratic functions modulus approach can effectively demonstrate the hydrodynamic idea of cross-flow drag at high angles of incidence, as it offers certain advantages.

Non-linear forces and moments were computed using the quadratic form to depict the non-linear forces on a ship hull (Fedyaevsky and Sobolev, 1963b). An accurate representation was achieved by incorporating lateral force caused by drag from the cross-flow velocity component. Nevertheless, the distribution of non-linear forces appeared to be more focused towards the stern.

The linear whole ship model gave accurate predictions for small rudder movements but proved to be inaccurate for complete turning circles (Yang, Chillcce, and El Moctar, 2023). In contrast, the non-linear whole ship model accurately depicted the three degrees of freedom motion in various manoeuvring scenarios, as validated by full-scale trials.

Inoue (1978) suggested using a combination of cubic and quadratic terms to incorporate non-linear factors. While the improvement was marginal, the cubic model showed a slightly better fit to the data compared to the quadratic model. There is a noticeable distinction between the two models, indicating a need for further investigation to refine mathematical representations of hydrodynamic forces.

The hydrodynamic derivatives are also important in other manoeuvring performances such as berthing (Zhang *et al.,* 2023), the interaction between ships (Degrieck *et al*., 2021), shallow water effect (Yang, and el Moctar, 2024), and so on. (Shouji and Ohtsu, 1992) used the quadratic polynomial to express the hydrodynamic forces and moment acting on a main hull induced by manoeuvring motion and (Sawada *et al.,* 2021) applied the cross-flow drag theory introduced by (Yoshimura, Nakao, and Ishibashi, 2009) to describe the hydrodynamic forces resulting from significant drift angles at low speeds. This model, which relies on fewer hydrodynamic derivatives than the traditional polynomial model, can effectively capture forces in both the transverse and turning directions. Furthermore, linearized hydrodynamic derivatives, as outlined by (Yasukawa and Sakuno, 2019). It can be used to calculate a ship's course stability index.

This research will focus on a mathematical model based on a polynomial model in order to investigate the differences between 3rd order polynomial (cubic model) and 2nd order polynomial (quadratic model). Additionally, when comparing the cubic model and the quadratic model, it is commonly believed that the cubic model is more effective in accurately estimating hydrodynamic force, especially in cases of large motion. However, it is important to note that the cubic model does not include a term that is proportional to the square of the drift angle. This omission may seem inconsistent with theoretical studies. However, despite this drawback, the cubic model is still preferred due to its ability to effectively explain physical phenomena. As a result, various research institutes may use different models, including the selection of sway velocity v'.

In this research, the measurement data of the hydrodynamic forces of 12 model vessels (total of 27 loading conditions) that had been conducted for turning tests and the zigzag tests in the past at Kyushu University were targeted. The β based second-order model and the v' based third order models are applied for re-analysis, and the results of a comparative study on the difference and approximation characteristics of the hydrodynamic force due to the difference of the adopted models are shown.

2. Mathematical models for lateral force and yawing moment

The dimensionless equations for manoeuvring motions can be described using equation (1) by taking into account the hull, propeller, and rudder components as follows,

$$\left.\begin{aligned} X' &= X'_H + X'_P + X'_R, \\ Y' &= Y'_H + Y'_P + Y'_R, \\ N' &= N'_H + N'_P + N'_R. \end{aligned}\right\} \tag{1}$$

The subscripts "H", "P" and "R" represent the hydrodynamic forces that have been non-dimensionalized and are acting on a hull, propeller, and rudder. In this study, particular focus is placed on investigating the lateral force Y'_H and yawing moment N'_H, as they have a significant impact on the accuracy of predicting manoeuvring.

Moreover, the hydrodynamic forces and moments experienced by a ship are dependent on its motion and are impacted by variables such as the ship's dimensions and type of movement. As a result, numerous parameters are needed to accurately describe these forces. The Taylor series expansion method can be used to simplify the complex characteristics of hydrodynamic forces into a mathematical equation with multiple variables. It is important for the hydrodynamic forces and their derivatives to be continuous and not approach infinity within the range of values. This requirement is typically met when analyzing hydrodynamic bodies like ships.

Additionally, the Taylor expansion is structured in a specific way as expressed in equation (2) when dealing with multiple variables.

$$f(x_1, \dots, x_k) = \sum_{a=0}^{n} \frac{1}{a!} \left(\Delta x_1 \partial_{x_1} + \cdots + \Delta x_k \partial_{x_k}\right)^n f((x_1)_0, \dots, (x_k)_0). \tag{2}$$

The combination of dimensionless sway velocity $v'(= v/U)$ and dimensionless yaw rate r' or a combination of drift angle $\beta(\simeq \sin\beta = -v')$ are frequently utilized as the variables such as $x_1, \cdots, x_k$.

$$\begin{aligned} f(v', r') = &\left[e^{\Delta_{v'}\partial_{v'} + \Delta_{r'}\partial_{r'} + \Delta^2_{v'}\Delta_{r'}\partial_{v'v'r'} + \Delta_{v'}\Delta^2_{r'}\partial_{v'r'r'} + \Delta^3_{v'}\partial_{v'v'v'} + \Delta^3_{r'}\partial_{r'r'r'}}\right] \\ &\times f\left[v'_0, r'_0, {v'_0}^2 r'_0, v'_0 {r'_0}^2, {v'_0}^3, {r'_0}^3\right], \end{aligned} \tag{3}$$

or,

$$\begin{aligned} f(\beta, r') = &\left[e^{\Delta_\beta\partial_\beta + \Delta_{r'}\partial_{r'} + \Delta^2_\beta\Delta_{r'}\partial_{\beta\beta r'} + \Delta_\beta\Delta^2_{r'}\partial_{\beta r'r'} + \Delta^3_\beta\partial_{\beta\beta\beta} + \Delta^3_{r'}\partial_{r'r'r'}}\right] \\ &\times f\left[\beta_0, r'_0, \beta_0^2 r'_0, \beta_0 {r'_0}^2, \beta_0^3, {r'_0}^3\right], \end{aligned} \tag{4}$$

The terms involving $v'r'$ (or $\beta r'$), ${v'}^2$ squared (or β^2), ${r'}^2$ squared, and other terms of a higher order are usually ignored. since their impact is considered less significant compared to the terms outlined in Equations (3) and (4). Alternatively, the hydrodynamic forces acting on a ship hull can be represented by equation (5) and (6) with second order polynomials as follows,

$$f(v',r') = \left[e^{\Delta_{v'}\partial_{v'}+\Delta_{r'}\partial_{r'}+\Delta_{v'}^{2}\partial_{v'v'}+\Delta_{r'}^{2}\partial_{r'r'}+\Delta_{v'}^{2}\Delta_{r'}\partial_{v'v'r'}+\Delta_{v'}\Delta_{r'}^{2}\partial_{v'r'r'}}\right] \times f\left[v_0', r_0', {v_0'}^2, {r_0'}^2, {v_0'}^2 r_0', v_0' {r_0'}^2\right], \tag{5}$$

or,

$$f(\beta,r') = \left[e^{\Delta_{\beta}\partial_{\beta}+\Delta_{r'}\partial_{r'}+\Delta_{\beta}^{2}\partial_{\beta\beta}+\Delta_{r'}^{2}\partial_{r'r'}+\Delta_{\beta}^{2}\Delta_{r'}\partial_{\beta\beta r'}+\Delta_{\beta}\Delta_{r'}^{2}\partial_{\beta r'r'}}\right] \times f\left[\beta_0, r_0', \beta_0^2, {r_0'}^2, \beta_0^2 r_0', \beta_0 {r_0'}^2\right]. \tag{6}$$

Just like with 3rd order polynomials, the coupling term $v'r'$ (or $\beta r'$) and other higher order terms are typically not taken into account. As a result, mathematical models that rely on the Taylor series around v' (or β) and r' are commonly presented in equation (7) and (8),

$$\left.\begin{aligned} Y_H' &= Y_v'v' + Y_r'r' + Y_{NL}'(v',r'), \\ N_H' &= N_v'v' + N_r'r' + N_{NL}'(v',r'), \end{aligned}\right\} \tag{7}$$

or,

$$\left.\begin{aligned} Y_H' &= Y_v'v' + Y_r'r' + Y_{NL}'(\beta,r'), \\ N_H' &= N_v'v' + N_r'r' + N_{NL}'(\beta,r'), \end{aligned}\right\} \tag{8}$$

Y_v', Y_r', N_v' and N_r' $\left(Y_\beta', Y_r', N_\beta'\right.$ and $\left.N_r'\right)$ represents linear hydrodynamic derivatives, while Y_{NL}' and N_{NL}' refer to nonlinear terms. The composition of linear terms, as depicted by the functions of v' (or β) and r', and their positions in the nonlinear terms vary among various research institutions.

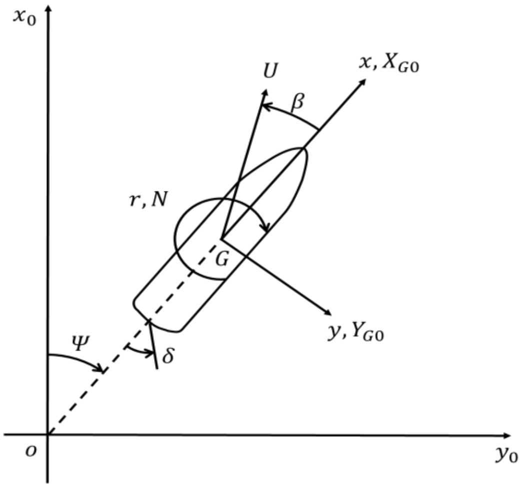

Figure 1 Ship manoeuvring motion in a body fixed coordinate system

The 3rd order model, which utilizes dimensionless sway velocity v' (Yasukawa and Yoshimura, 2015), is represented by equations in the ship fixed coordinate system $G - xy$ displayed in Figure 1.

$$\left.\begin{aligned} Y_H' &= Y_v'v' + Y_r'r' + Y_{vvv}'v'^3 + Y_{vvr}'v'^2r' + Y_{vrr}'v'r'^2 + Y_{rrr}'r'^3, \\ N_H' &= N_v'v' + N_r'r' + N_{vvv}'v'^3 + N_{vvr}'v'^2r' + N_{vrr}'v'r'^2 + N_{rrr}'r'^3. \end{aligned}\right\} \tag{9}$$

Y_H' and N_H' Illustrate the dimensionless values of lateral force and yawing moment. Kyushu University traditionally uses a second order model based on drift angle β (Kijima *et al.,* 1990), which is represented by the equations below

$$\left.\begin{aligned} Y'_H &= Y'_\beta \beta + Y'_r r' + Y'_{\beta\beta}\beta|\beta| + Y'_{rr} r'|r'| + \left(Y'_{\beta\beta r}\beta + Y'_{\beta rr} r'\right)\beta r' \,, \\ N'_H &= N'_\beta \beta + N'_r r' + N'_{\beta\beta}\beta|\beta| + N'_{rr} r'|r'| + \left(N'_{\beta\beta r}\beta + N'_{\beta rr} r'\right)\beta r' . \end{aligned}\right\} \tag{10}$$

The 2nd order model terms of β and r' contain absolute symbols, signifying hydrodynamic force changes based on motion direction. The model in Equation (9) is referred to as the "cubic model", while the model in Equation (10) is known as the "quadratic model".

Table 1 Ship models principal dimensions

Ship No.	Ship Type	Ship Name	Loading Condition	β (deg.)	r'	L (m)	B (m)	d_m (m)	C_B
1 2	Container C.	SR108	Full Ballast	-4.0~ 12.0	0 ~ 0.5454	3.0	0.435	0.163 0.094	0.572 0.518
3 4	VLCC	Esso Osaka	Full Ballast	-4.0~ 20.0	0 ~ 0.8000	2.5	0.408	0.170 0.080	0.831 0.793
5 6	Car C.	Ship A	Full Ballast	-4.0~ 10.0	0 ~ 0.9615	2.5	0.482	0.134 0.111	0.522 0.491
7 8	Cargo C.	Ship B	Full Ballast	-4.0~ 10.0	0 ~ 0.9615	2.5	0.419	0.140 0.082	0.698 0.666
9 10	ULCC	Ship C	Full Ballast	-4.0~ 20.0	0 ~ 0.9615	2.5	0.466	0.156 0.076	0.835 0.802
11 12 13	LNG C.	Ship D	Full Half Ballast	-4.0~ 20.0	0 ~ 0.9615	2.5	0.409	0.100 0.093 0.086	0.714 0.707 0.703
14 15	VLCC	Ship E	Full Ballast	-4.0~ 20.0	0 ~ 1.0000	2.5	0.436	0.157 0.077	0.802 0.761
16 17 18	Container C.	Ship F	Full Half Ballast	-4.0~ 20.0	0 ~ 0.9615	2.5	0.386	0.130 0.107 0.085	0.566 0.540 0.516
19 20	Cargo C.	Ship G	Full Ballast	-4.0~ 20.0	0 ~ 0.9615	2.5	0.376	0.158 0.072	0.651 0.574
21 22	Cargo C.	Ship H	Full Ballast	-4.0~ 20.0	0 ~ 0.9615	2.5	0.408	0.171 0.071	0.773 0.711
23 24 25	RO/RO	Ship I	Full Half Ballast	-4.0~ 20.0	0 ~ 0.9615	2.5	0.367	0.102 0.093 0.083	0.557 0.537 0.512
26 27	ULCC	Ship J	Full Ballast	-4.0~ 20.0	0 ~ 0.9615	2.5	0.556	0.183 0.089	0.821 0.783

The hydrodynamic forces from captive model tests were reanalyzed for 12 different model ships. This analysis was based on the mathematical models in Equations (9) and (10), in order to determine the hydrodynamic derivatives. Table 1 provides details on the ships, including the range of drift angle β, length L, width B, average draft d_m, and block coefficient C_B. SR108 and Esso Osaka are known for their widely disclosed hull shape and experimental data. Ships A to J were used as test ships, with measurement data available for fully loaded, ballast, and, in some cases, half-loaded conditions. Table 2 and Table 3 shows the determined hydrodynamic derivatives based on cubic model and quadratic model respectively.

Table 2 Cubic model hydrodynamic derivatives

Ship No.	Y'_v	Y'_{vvv}	Y'_r	Y'_{rrr}	Y'_{vrr}	Y'_{vvr}	N'_v	N'_{vvv}	N'_r	N'_{rrr}	N'_{vrr}	N'_{vvr}
1	0.234	3.272	-0.119	0.020	1.128	0.012	0.111	-0.288	-0.044	-0.047	-0.083	-0.579
2	0.202	2.073	-0.124	0.051	0.938	-0.268	0.062	-0.137	-0.030	-0.056	0.043	-0.554
3	0.430	1.452	-0.238	0.059	0.498	0.280	0.154	0.058	-0.071	-0.008	-0.117	-0.169
4	0.335	0.759	-0.235	0.016	0.376	0.134	0.079	0.075	-0.056	-0.011	-0.029	-0.187
5	0.346	2.437	-0.187	-0.109	1.085	-1.094	0.109	1.061	-0.069	-0.027	0.061	-0.605
6	0.317	7.566	-0.175	-0.097	0.811	-1.932	0.087	0.723	-0.063	-0.032	0.115	-0.684
7	0.320	4.768	-0.109	-0.060	0.521	-0.831	0.108	-0.088	-0.054	-0.024	-0.054	-0.228
8	0.229	3.252	-0.110	-0.165	0.830	-0.878	0.066	-0.088	-0.045	-0.017	0.057	-0.366
9	0.479	0.975	-0.269	-0.025	0.270	0.569	0.134	0.023	-0.055	-0.013	-0.018	-0.177
10	0.371	0.613	-0.247	-0.055	0.202	0.182	0.065	0.099	-0.043	-0.005	0.007	-0.168
11	0.359	0.948	-0.203	-0.005	0.281	0.153	0.076	-0.003	-0.044	-0.007	-0.017	-0.147
12	0.333	0.644	-0.193	-0.028	0.281	0.192	0.070	0.018	-0.042	-0.006	-0.006	-0.148
13	0.321	0.574	-0.193	-0.017	0.259	0.234	0.067	-0.033	-0.037	-0.010	-0.008	-0.116
14	0.381	1.559	-0.221	0.023	0.531	0.047	0.127	0.012	-0.059	-0.013	-0.099	-0.164
15	0.321	0.591	-0.205	-0.018	0.277	0.303	0.065	0.087	-0.046	-0.018	-0.030	-0.137
16	0.280	3.498	-0.101	-0.055	1.036	-1.891	0.093	0.089	-0.048	-0.040	0.012	-0.350
17	0.281	2.177	-0.093	-0.070	0.903	-1.246	0.076	0.067	-0.043	-0.042	0.073	-0.410
18	0.284	2.156	-0.089	-0.078	0.829	-1.215	0.063	0.169	-0.035	-0.042	0.076	-0.462
19	0.354	2.167	-0.155	-0.009	0.897	-0.901	0.125	0.095	-0.058	-0.041	-0.066	-0.275
20	0.247	1.034	-0.128	-0.035	0.600	-0.478	0.056	0.086	-0.031	-0.036	0.043	-0.341
21	0.295	2.470	-0.176	-0.023	0.546	-0.129	0.145	-0.157	-0.047	-0.026	-0.120	-0.135
22	0.320	0.484	-0.199	-0.031	0.283	0.273	0.064	-0.062	-0.038	-0.015	-0.072	-0.021
23	0.238	2.196	-0.124	-0.073	0.854	-1.486	0.075	0.213	-0.035	-0.033	0.123	-0.564
24	0.231	2.003	-0.144	-0.020	0.781	-1.259	0.067	0.199	-0.032	-0.039	0.146	-0.601
25	0.215	2.672	-0.124	-0.056	0.917	-1.733	0.058	0.322	-0.034	-0.041	0.166	-0.663
26	0.476	1.538	-0.278	-0.031	0.269	0.492	0.151	0.139	-0.056	-0.024	-0.056	-0.201
27	0.352	0.458	-0.285	-0.018	0.109	0.482	0.071	0.115	-0.048	-0.008	0.006	-0.215

Table 3 Quadratic model hydrodynamic derivatives

Ship No.	Y'_β	$Y'_{\beta\beta}$	Y'_r	Y'_{rr}	$Y'_{\beta rr}$	$Y'_{\beta\beta r}$	N'_β	$N'_{\beta\beta}$	N'_r	N'_{rr}	$N'_{\beta rr}$	$N'_{\beta\beta r}$
1	0.179	0.899	-0.124	0.021	1.280	-0.427	0.118	-0.093	-0.034	-0.044	-0.151	-0.384
2	0.163	0.591	-0.135	0.049	0.994	-0.451	0.065	-0.047	-0.019	-0.052	-0.007	-0.410
3	0.372	0.601	-0.251	0.060	0.547	0.138	0.155	0.007	-0.068	-0.011	-0.128	-0.140
4	0.294	0.344	-0.240	0.020	0.404	0.049	0.074	0.034	-0.052	-0.013	-0.033	-0.174
5	0.409	-0.008	-0.141	-0.151	1.244	-1.771	0.091	0.279	-0.056	-0.041	0.073	-0.744
6	0.274	1.484	-0.132	-0.136	0.930	-2.716	0.073	0.203	-0.047	-0.048	0.125	-0.768
7	0.272	1.060	-0.082	-0.085	0.500	-0.719	0.110	-0.029	-0.043	-0.034	-0.088	-0.018
8	0.197	0.712	-0.043	-0.225	0.871	-1.143	0.068	-0.027	-0.038	-0.023	0.064	-0.399
9	0.435	0.405	-0.257	-0.037	0.277	0.541	0.136	-0.004	-0.049	-0.019	-0.023	-0.155
10	0.345	0.248	-0.223	-0.077	0.240	0.077	0.061	0.039	-0.041	-0.007	0.005	-0.157
11	0.323	0.383	-0.199	-0.009	0.279	0.146	0.076	-0.005	-0.040	-0.010	-0.012	-0.158
12	0.300	0.285	-0.179	-0.042	0.250	0.261	0.068	0.006	-0.040	-0.008	-0.011	-0.134
13	0.288	0.262	-0.185	-0.024	0.260	0.216	0.069	-0.019	-0.033	-0.013	-0.014	-0.093
14	0.305	0.695	-0.231	0.032	0.604	-0.185	0.125	0.003	-0.052	-0.020	-0.115	-0.111
15	0.297	0.236	-0.197	-0.025	0.302	0.220	0.061	0.035	-0.038	-0.026	-0.031	-0.126
16	0.127	1.530	-0.079	-0.075	1.093	-2.077	0.089	0.035	-0.029	-0.057	-0.006	-0.283

Table 3 Quadratic model hydrodynamic derivatives (Cont.)

Ship No.	Y'_β	$Y'_{\beta\beta}$	Y'_r	Y'_{rr}	$Y'_{\beta rr}$	$Y'_{\beta\beta r}$	N'_β	$N'_{\beta\beta}$	N'_r	N'_{rr}	$N'_{\beta rr}$	$N'_{\beta\beta r}$
17	0.180	0.969	-0.064	-0.096	0.926	-1.321	0.073	0.026	-0.025	-0.060	0.065	-0.373
18	0.185	0.953	-0.057	-0.106	0.876	-1.345	0.056	0.071	-0.016	-0.059	0.067	-0.417
19	0.263	0.930	-0.148	-0.016	0.957	-1.111	0.123	0.027	-0.039	-0.059	-0.071	-0.241
20	0.203	0.441	-0.112	-0.051	0.624	-0.563	0.053	0.033	-0.014	-0.052	0.025	-0.282
21	0.179	1.102	-0.167	-0.032	0.591	-0.305	0.156	-0.091	-0.035	-0.038	-0.139	-0.064
22	0.307	0.170	-0.185	-0.045	0.276	0.271	0.069	-0.037	-0.031	-0.021	-0.085	0.021
23	0.143	0.956	-0.093	-0.101	0.851	-1.487	0.065	0.095	-0.020	-0.047	0.092	-0.461
24	0.140	0.890	-0.133	-0.031	0.748	-1.170	0.059	0.082	-0.015	-0.055	0.121	-0.509
25	0.092	1.192	-0.097	-0.081	0.943	-1.806	0.044	0.139	-0.016	-0.059	0.152	-0.605
26	0.416	0.633	-0.264	-0.044	0.300	0.371	0.147	0.045	-0.046	-0.034	-0.063	-0.173
27	0.334	0.179	-0.277	-0.025	0.112	0.445	0.067	0.043	-0.044	-0.011	0.001	-0.194

3. Results and Discussion

3.1. Comparison of approximation accuracy of hydrodynamic force

Y'_H and N'_H are calculated using hydrodynamic derivatives which were obtained based on Equations (9) and (10). The accuracy of predicted hydrodynamic force was compared based on the coefficient of determination R^2 defined by equation (11).

$$R^2 = 1 - \frac{\sum(y_i - f_i)^2}{\sum(y_i - y_m)^2} \tag{11}$$

Here, y_i is the measured value of Y'_H or N'_H, y_m is the average value of the measured data, and f_i is the value calculated by Equation (9) or Equation (10). The closer the value of R^2 to 1.0, the better the approximation accuracy results. Figure 2 compares R^2 values of the cubic model and quadratic model for every ship and their loading conditions are shown in Table 1. Ship numbers (1-27) in Table 1 are shown on the horizontal axis. The lines connecting each point are added for convenience and have no physical meaning. For both Y'_H and N'_H, R^2 values of the cubic model are generally closer to 1, indicating that the approximation accuracy of the cubic model is generally better than that of the quadratic model. Looking at the lateral force, the differences in the R^2 values of Ship No. 5 to 8 (Ships A and B) are particularly large. For these model ships and loading conditions, as shown in Table 1, the maximum value of the drift angle at which the hydrodynamic force was measured is 10°. Figure 3 shows the comparison between ship No. 8 and ship No. 22, which have the same type of ship and loading condition. A large difference appears in the calculation results of ship No. 8 based on both models within a wide range of drift angles.

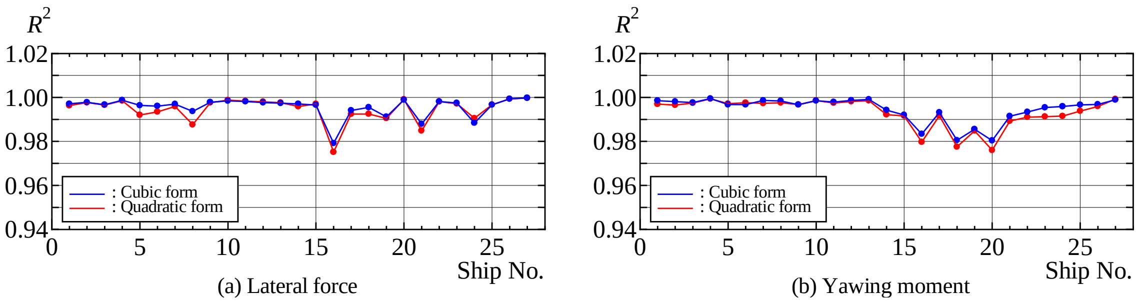

Figure 2 Comparison of the R^2 value for cubic and quadratic models (a) lateral force and (b) yawing moment

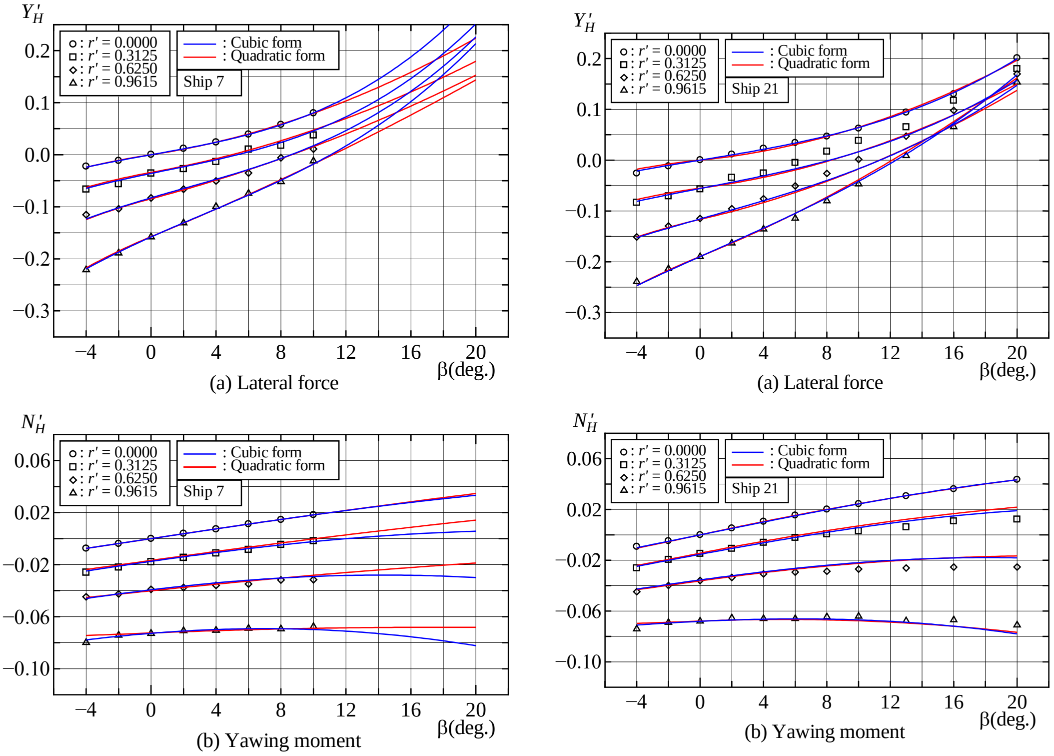

Figure 3 Comparison of lateral force and yawing moment by cubic and quadratic models for ship B (a) and Ship H (b) on fully loaded condition

On the other hand, for the yawing moment, there is a tendency for the differences in the values of R^2 to increase model ships and loading conditions after Ship No. 14. The comparison between Ship No. 3 and Ship No. 14 is shown in Figure 4. Both of these ships have the same type and loading condition. From the figures, the nonlinearity with respect to β appears to be large when r' is large.

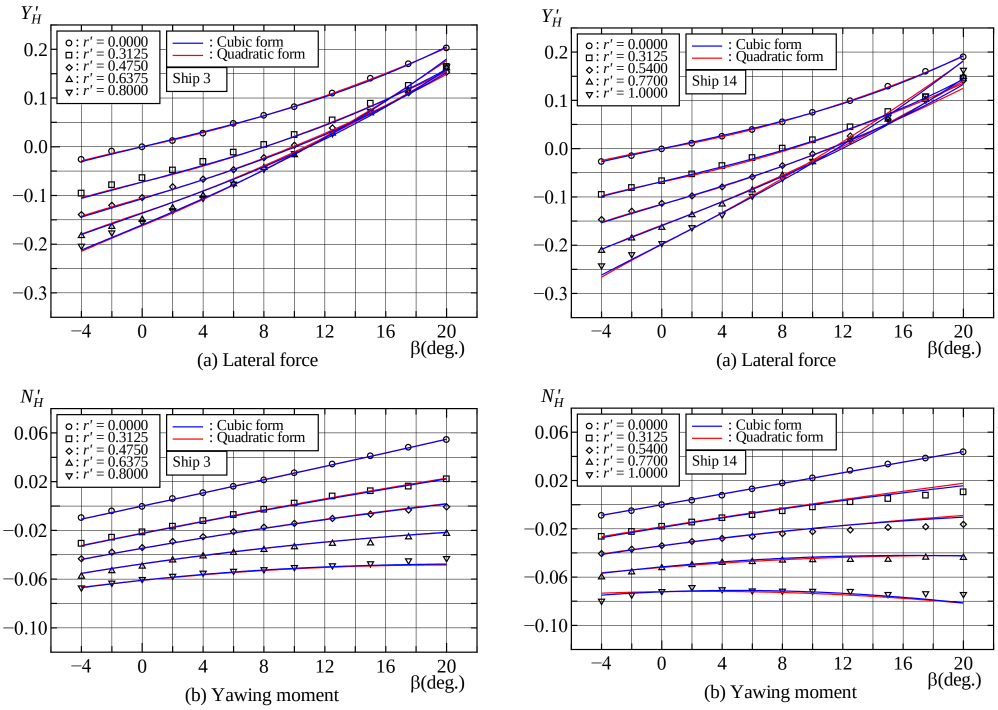

Figure 4 Comparison of Y'_H and N'_H by cubic and quadratic models for Esso Osaka (a) and Ship E (b) on fully loaded condition

3.2. Effect of measurement range of drift angle β on approximation accuracy

To clarify the cause of the differences in approximation accuracy shown in Figure 2, the range of drift angle used to calculate the hydrodynamic derivatives was changed and the analysis was performed again. The influence of the drift angle measurement range on the hydrodynamic forces' approximation accuracy was investigated.

First, for model ships and loading conditions shown as Ships No. 1 to 4 and Ships No. 9 to 27 whose hydrodynamic forces were measured in the range of $\beta > 10^{\circ}$, the range of the measured hydrodynamic forces data used in the analysis was limited to $\beta \leq 10^{\circ}$. After the hydrodynamic derivatives were obtained, the calculated results of lateral force and yaw moment were compared with the original results. For example, Figure 5 shows the results for the Esso Osaka (Ship No. 3) in fully loaded condition. The figures also show the measurement data in the range of $\beta > 10^{\circ}$, that were not used in the analysis.

In Figure 5 (right), regarding the lateral forces, there is a large difference between the calculation results of both mathematical models in the range where the value of β is large. As the value of β increases, the cubic model tends to exhibit a higher rate of increase for lateral force. Consequently, there is a widening discrepancy between the calculated results and the measured values. Conversely, for the yaw moment, it appears that the quadratic model yields better results when the turning motion is minimal (when the value of r' is small). However, as the turning motions develop, the cubic model has better agreement with the measured values.

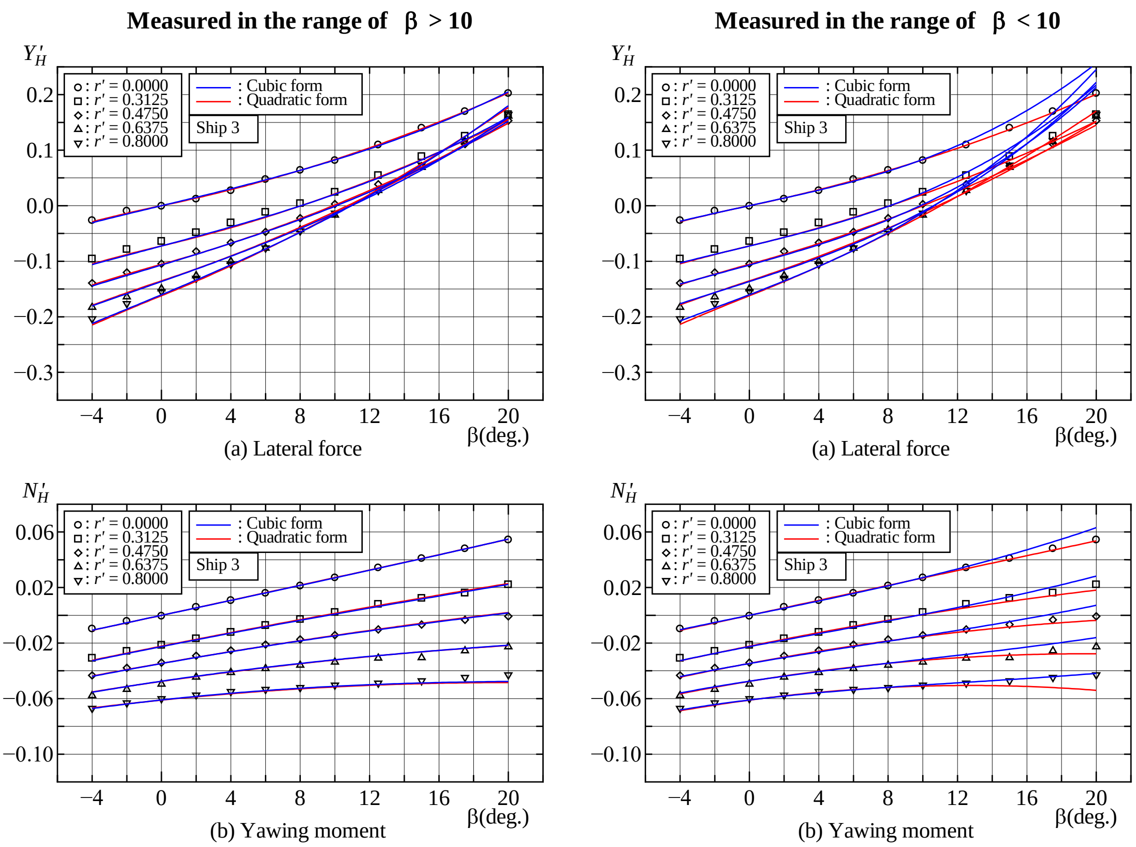

Figure 5 Comparison of Y_H' and N_H' by both mathematical models for Esso Osaka on fully loaded condition in the range of $\beta > 10^{\circ}$ (a) and $\beta < 10^{\circ}$ (b)

Next, Lateral force and yaw moment were determined for model ships and loading conditions of Ships No. 1 to 4 and Ships No. 9 to 27 using the hydrodynamic derivatives obtained from the measurement data of $\beta \leq 10^{\circ}$, Figure 6 shows the values of R^2 including the measured data for $\beta > 10^{\circ}$. For lateral force, the quadratic model maintains the values of R^2 close to 1.0 in many model ships and loading conditions, whereas the cubic model has a lower value of R^2 compared to Figure 2. Although it was shown in Figure 2 that R^2 values of the cubic model for Ships No. 5 to 8 have good approximation accuracy in the range of $\beta \leq 10^{\circ}$, it may be necessary to be careful when applying the conditions of motion outside the measurement range. On the other hand, the influence of the measurement range of β on approximation accuracy of the hydrodynamic forces using the quadratic model is considered relatively small. There is no significant difference in the yaw moment due to the difference between them.

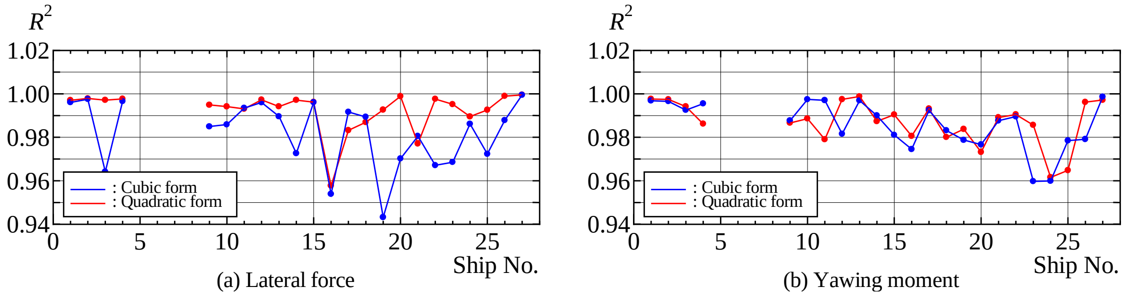

Figure 6 Comparison of the R^2 value for cubic and quadratic forms (a) lateral force; and (b) yawing moment

Finally, Figures. 7 and 8 show the results of hydrodynamic derivatives for lateral force and yaw moment as functions of parameters representing hull form. The symbol ■ indicates the hydrodynamic derivatives for Ships No. 5 to 8, and the symbol ○ indicates the hydrodynamic derivatives for other model ships and loading conditions. The parameters on the horizontal axis in each figure have the maximum value of R^2 when polynomial approximation of the corresponding hydrodynamic derivatives is performed using the parameters.

Looking at the linear hydrodynamic derivatives first, there is a linear relation between the derivatives and the parameters on the horizontal axis regardless of the ■ and ○ marks. On the other hand, when looking at the non-linear hydrodynamic derivatives, the variation is slightly larger than that of the linear derivatives. The symbol ■ which shows the hydrodynamic derivatives for Ships No. 5 to 8 shows tendency different from the symbol ○ which shows the hydrodynamic derivatives for other model ships and loading conditions, as mentioned above. It is considered that the narrow measurement range of the drift angle affects the analysis results.

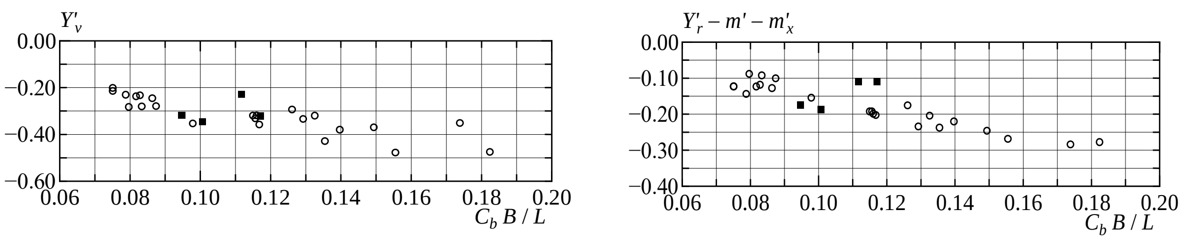

(a) (b)

Figure 7 Hydrodynamic derivatives for lateral force in cubic form as a function of hull form parameters (a) Y'_v; (b) $Y'_r - m' - m'_x$; (c) Y'_{vvv}; (d) Y'_{vvr}; (e) Y'_{vrr}; and (f) Y'_{rrr}

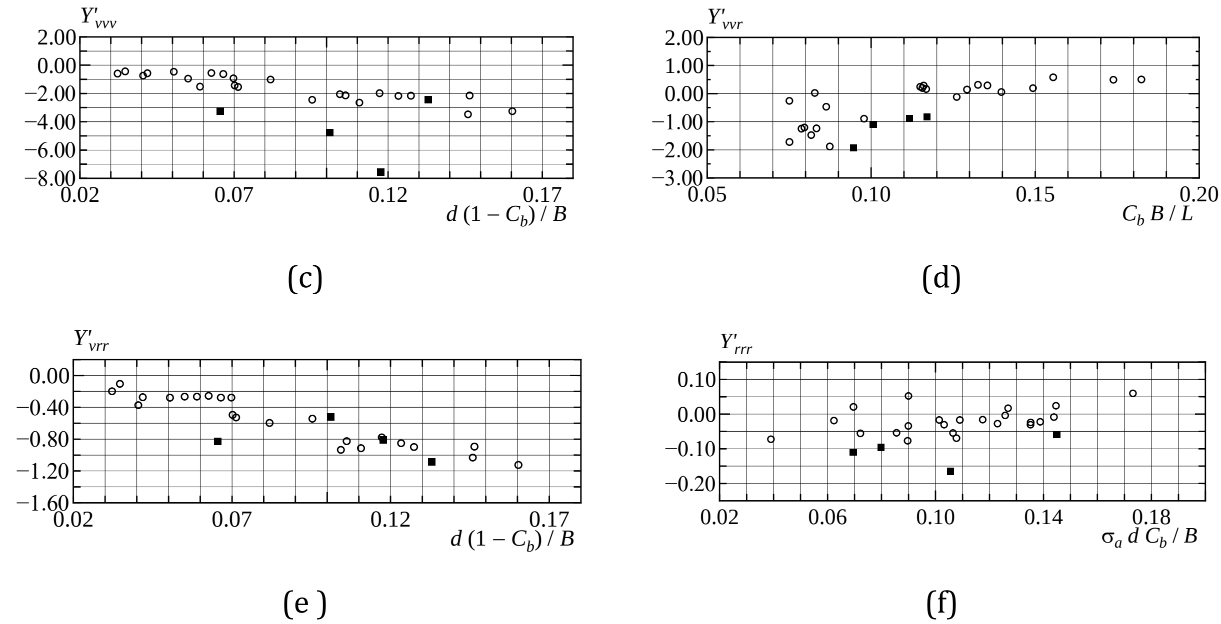

Figure 7 Hydrodynamic derivatives for lateral force in cubic form as a function of hull form parameters (a) Y'_v; (b) $Y'_r - m' - m'_x$; (c) Y'_{vvv}; (d) Y'_{vvr}; (e) Y'_{vrr}; and (f) Y'_{rrr} (Cont.)

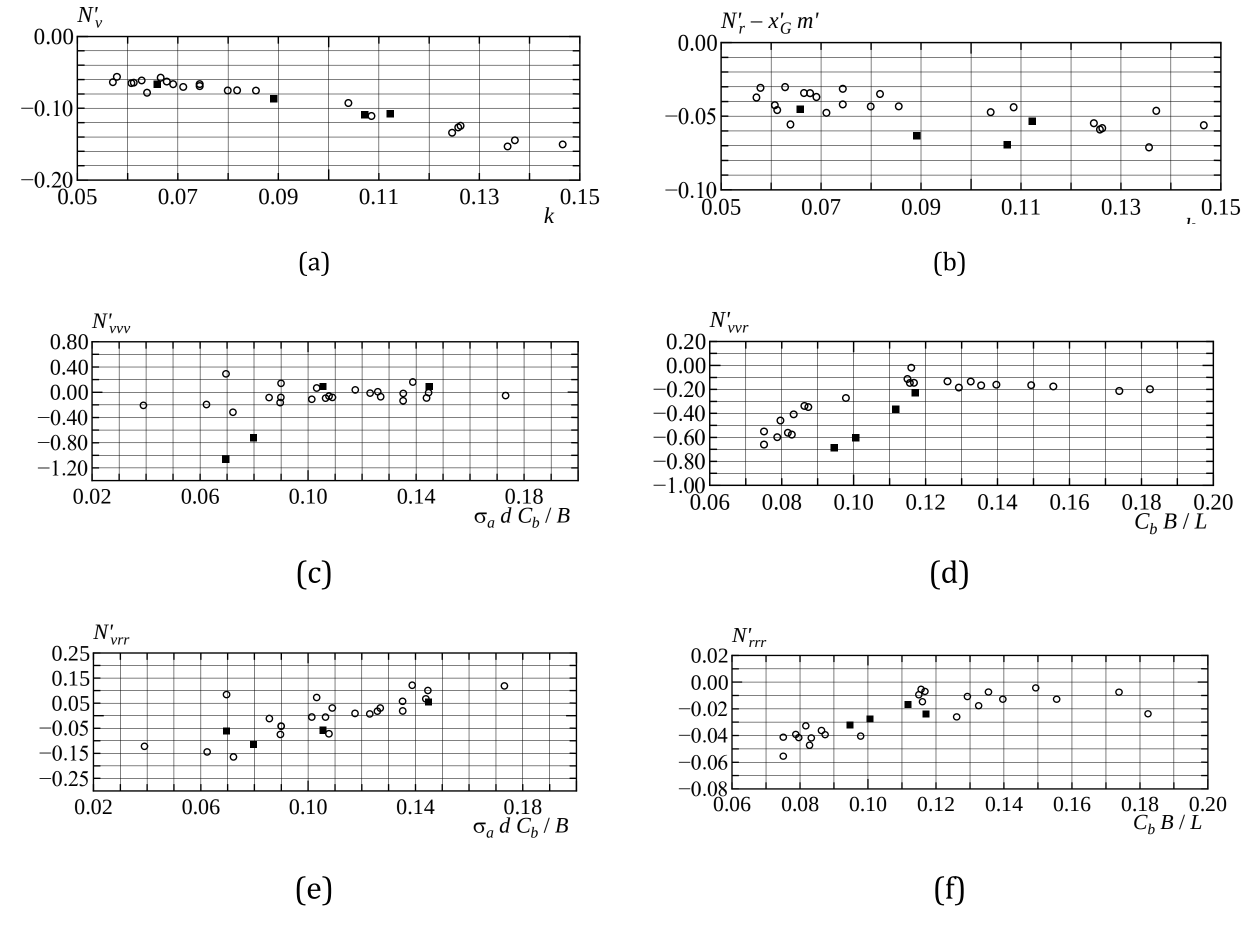

Figure 8 Hydrodynamic derivatives for yawing moment in cubic form as function of hull form parameters (a) N'_v; (b) $N'_r - x'_G m'$; (c) N'_{vvv}; (d) N'_{vvr}; (e) N'_{vrr}; and (f) N'_{rrr}

3.3. Course Stability Index

The course stability index (Δ) can be determined by using the linear hydrodynamic derivatives provided in Equations (9) and (10) (Yoshimura, 2001; Yukawa and Kijima, 1998).

$$\Delta = -Y_v' N_r' + N_v'\{Y_r' - (m' + m_x')\} = Y_\beta' N_r' - N_\beta'\{Y_r' - (m' + m_x')\}. \tag{12}$$

Here, a positive (+) Δ indicates instability, while a negative (-) Δ indicates stability. Then, Equation (12) can be rewritten to equation (13)-(15),

$$\begin{aligned}\Delta &= -Y_v'\{Y_r' - (m' + m_x')\}\left\{\frac{N_r'}{Y_r' - (m' + m_x')} - \frac{N_v'}{Y_v'}\right\} \\ &= -Y_v'\{Y_r' - (m' + m_x')\}(l_r' - l_v'),\end{aligned} \tag{13}$$

$$\begin{aligned}\Delta &= Y_\beta'\{Y_r' - (m' + m_x')\}\left\{\frac{N_r'}{Y_r' - (m' + m_x')} - \frac{N_\beta'}{Y_\beta'}\right\} \\ &= Y_\beta'\{Y_r' - (m' + m_x')\}(l_r' - l_\beta'),\end{aligned} \tag{14}$$

where,

$$l_r' = \frac{N_r'}{Y_r' - (m' + m_x')}, \qquad l_v' = \frac{N_v'}{Y_v'}, \qquad l_\beta' = \frac{N_\beta'}{Y_\beta'}. \tag{15}$$

l_r' represents the location where the yaw damping force is applied, while l_β' and l_v' represent the locations where the sway damping force is applied. The positions of these points where forces are applied relative to each other can be used to assess the course stability of a ship. The stability of a ship depends on the positioning of the yaw damping force application point relative to the sway damping force application point. The ship is considered to be stable when the point at which the yaw damping force is applied is located in front of the point where the sway damping force is applied. On the other hand, if this is not the case, the ship is considered unstable.

The course stability indices of the quadratic and cubic models are being compared to determine the impact of using different model approaches according to equations (12) to (15). Figure 9 illustrates the linear hydrodynamic derivatives derived from analyzing measured hydrodynamic forces using both models, which are then utilized in calculating the course stability indices.

Figure 10 presents a comparison of course stability indices between 2 mathematical models for different model ships and loading conditions as detailed in Table 1. The x-axis shows the number of ships ranging from 1 to 27. It is clear that some ships show differences in course stability indices when using both mathematical models. Several factors may contribute to this discrepancy, such as differences in the mathematical properties of each model.

To achieve a better comprehension of the phenomenon, the relationship between the Δ and the hydrodynamic derivatives of both mathematical models for each of the 27 ships are being analyzed. The ships are then categorized into three groups based on the results of calculated Δ for easier comprehension.

I. Ships with consistent Δ signs for cubic and quadratic models across all loading conditions.
II. Ships exhibit different Δ signs for cubic and quadratic models under certain loading conditions.
III. Ships exhibit different Δ signs for cubic and quadratic models across all loading conditions.

Figure 11 provides illustrations of the three categories, while Table 4 displays the breakdown of ships that fit into each category.

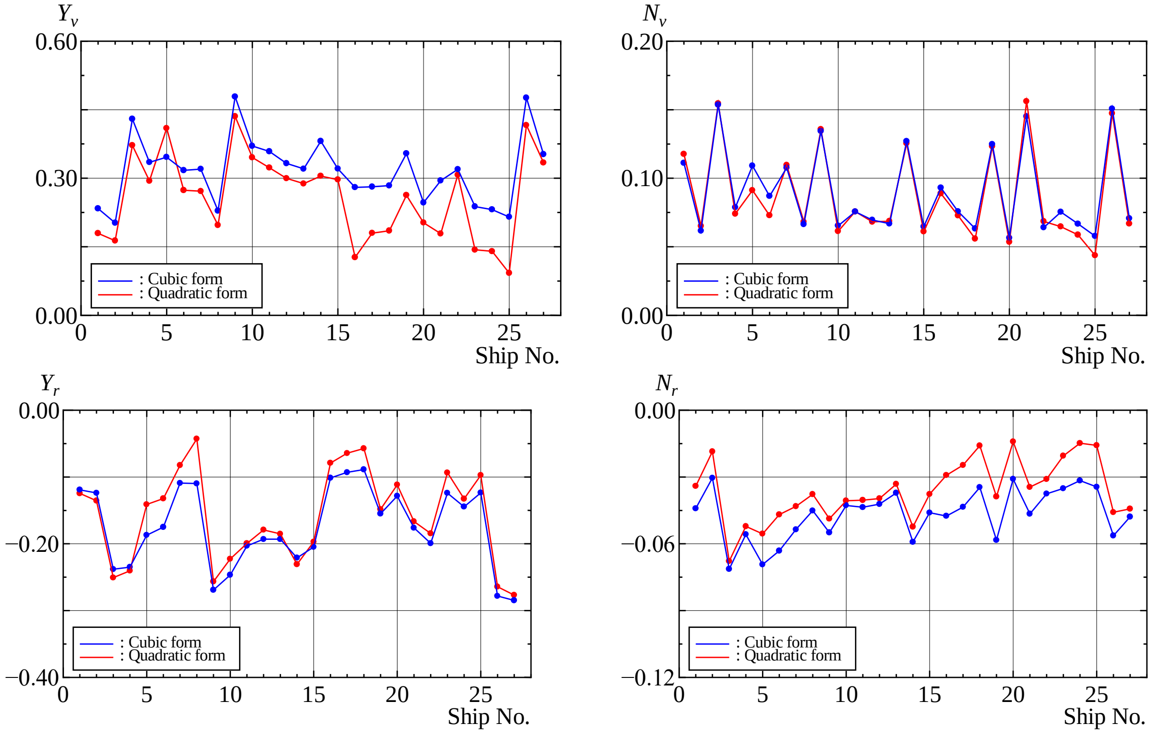

Figure 9 Linear hydrodynamic derivatives based on quadratic and cubic models

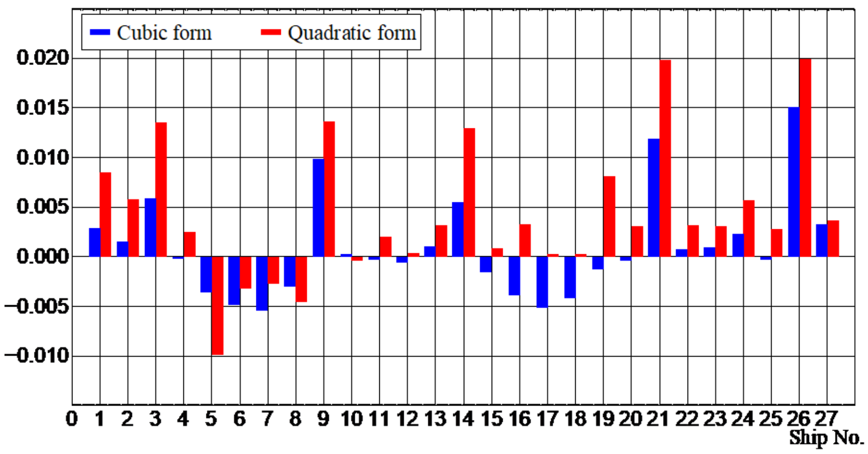

Figure 10 Quadratic model vs cubic model of Δ

Table 4 List of ships

Category 1	Category 2	Category 3
SR108	Esso Osaka	Ship F
Ship A	Ship C	Ship G
Ship B	Ship D	
Ship H	Ship E	
Ship J	Ship I	

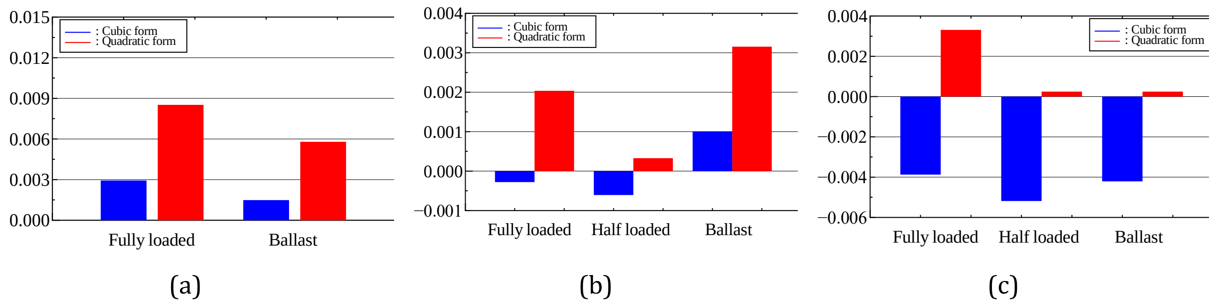

Figure 11 Examples of Δ for three different categories (a) Category 1 – SR108; (b) Category 2 – Ship C; and (c) Category 3 – Ship F

Figure 12 displays the Y'_H and N'_H curves of Ships No. 1 and 2 (SR108) under fully loaded and ballast conditions, fitted with cubic and quadratic models within the range of -$-10° < \beta < 20°$ at $r' = 0$. The red and blue solid lines on the graph represent fitting curves based on hydrodynamic derivatives from captive model test data, with the horizontal axis showing the drift angle β. The dashed lines on the graph indicate the inclines of the curves representing lateral force and yawing moment at the starting point, which are equivalent to linear hydrodynamic derivatives for β and are referred to as slope lines. The figures display experimental data points marked with circles. The slope of the cubic model for lateral force is steeper than that of the quadratic model, whereas the opposite is true for yawing moment. These trends are consistent across both loading conditions.

A noticeable distinction exists between the Y'_H and N'_H curves produced by cubic and quadratic models over a wide range of drift angles β. In general, when using the least square method to fit a curve with a cubic function, the resulting values tend to be larger beyond the input data range compared to fitting with a quadratic function. This discrepancy is attributed to the limited availability of experimental data for large drift angles.

Figure 13 displays the Y'_H and N'_H curves for Ship C (Ships No. 9 and 10) under ballast and fully loaded conditions in category 2. The discrepancy in Δ signs between the two ships are primarily due to variations in the yawing moment slope line in relation to drift angle β. Both ships exhibit a smaller inclination of the quadratic model slope line for lateral force compared to the cubic model. However, there is a contrasting trend in the yawing moment between Ship No. 9 and Ship No. 10, with Ship No. 9 showing a slightly larger inclination of the quadratic model slope line. This difference in tendencies is not observed in Category 1, where all Δ signs are consistent. The varying Δ signs are a result of differences in linear hydrodynamic derivatives between the two models, as detailed in Table 2 and Table 3.

In Category 3, Figure 14 displays the Y'_H and N'_H curves of Ships No. 16 and 18 (Ship F) under fully loaded and ballast conditions. The Y'_H and N'_H curves show no significant difference between fully loaded and ballast conditions. Yet, the slope line of the quadratic model is less steep compared to the cubic model when it comes to lateral force and yawing moment in relation to drift angle β. Conversely, the slope line inclination of the quadratic model for Y'_H and N'_H in relation to the r' is greater than that of the cubic model. This trend is also evident in Figure 9.

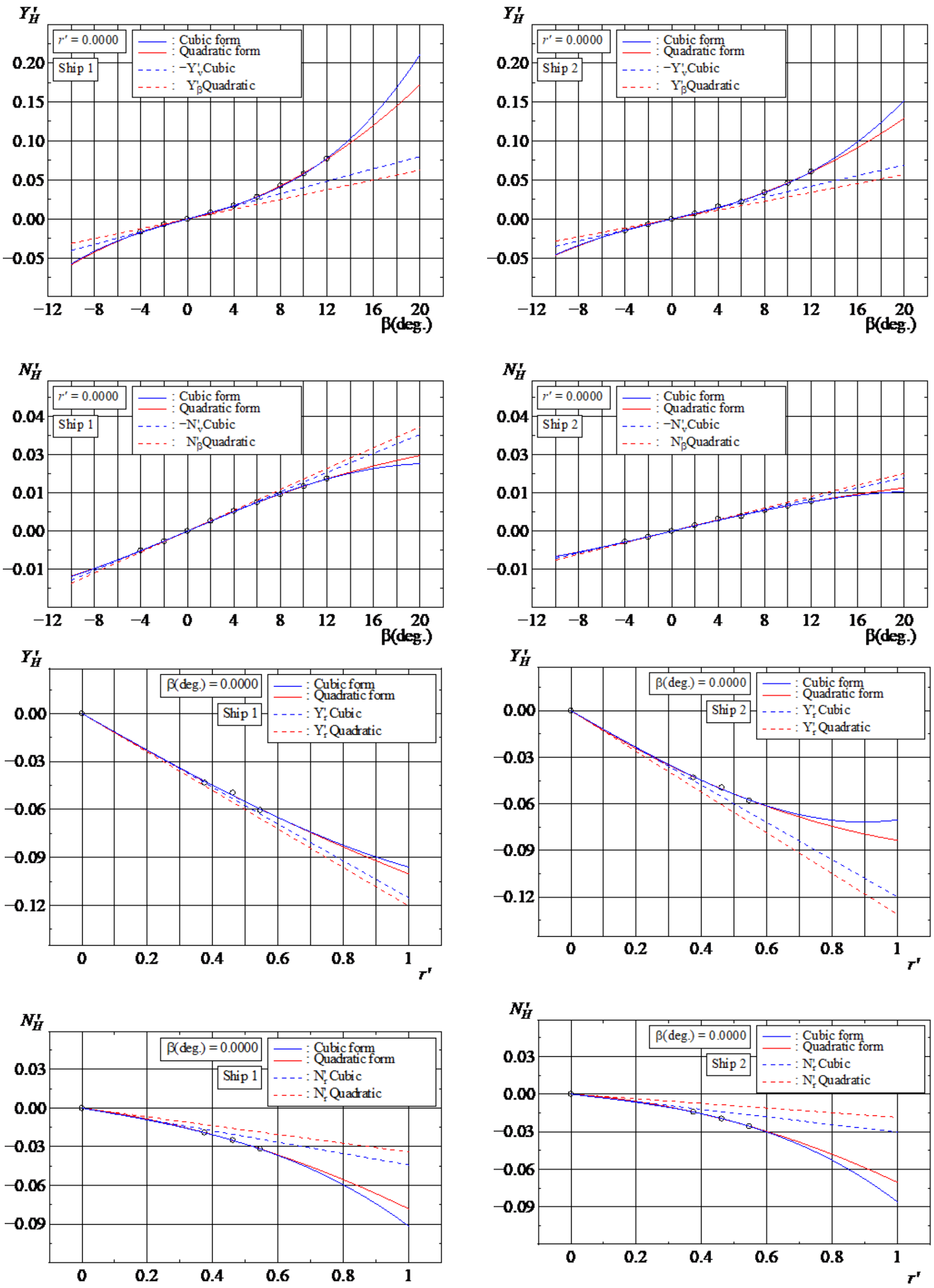

(a) (b)

Figure 12 Category 1 - The Y_H' and N_H' curves of SR108 were modelled for both loading conditions (a) Fully loaded condition and (b) Ballast condition

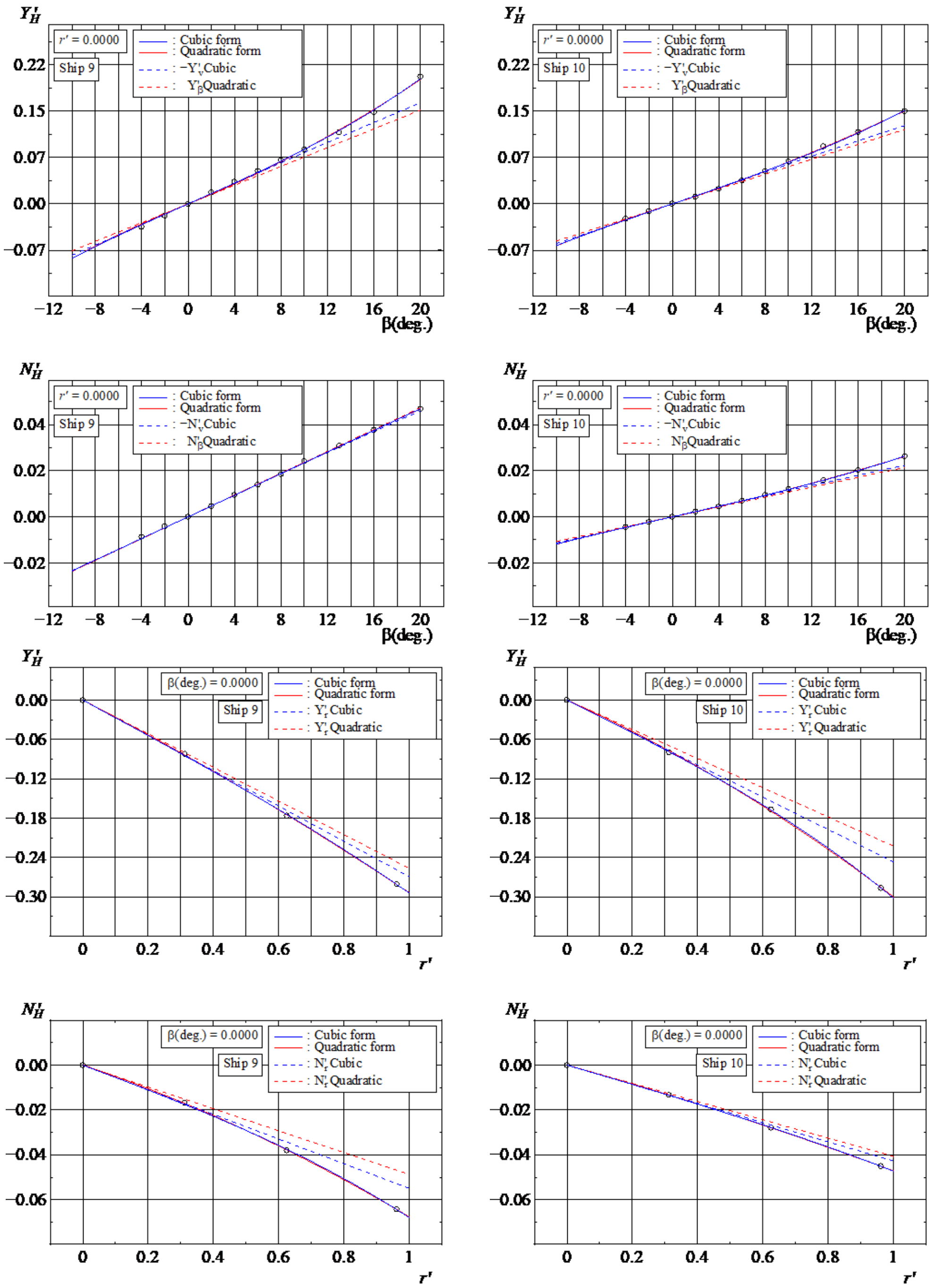

(a) (b)

Figure 13 Category 2 - The Y'_H and N'_H curves of Ship C were modeled for both loading conditions (a) Fully loaded condition and (b) Ballast condition

Previously, the focus was on comparing loading conditions to analyze the variation in hydrodynamic derivatives and Δ between both mathematical models of the same ship types. Many ships display a difference in Δ between the two models. Understanding the reasons behind these results is crucial. Consequently, ships within each category are being compared once more.

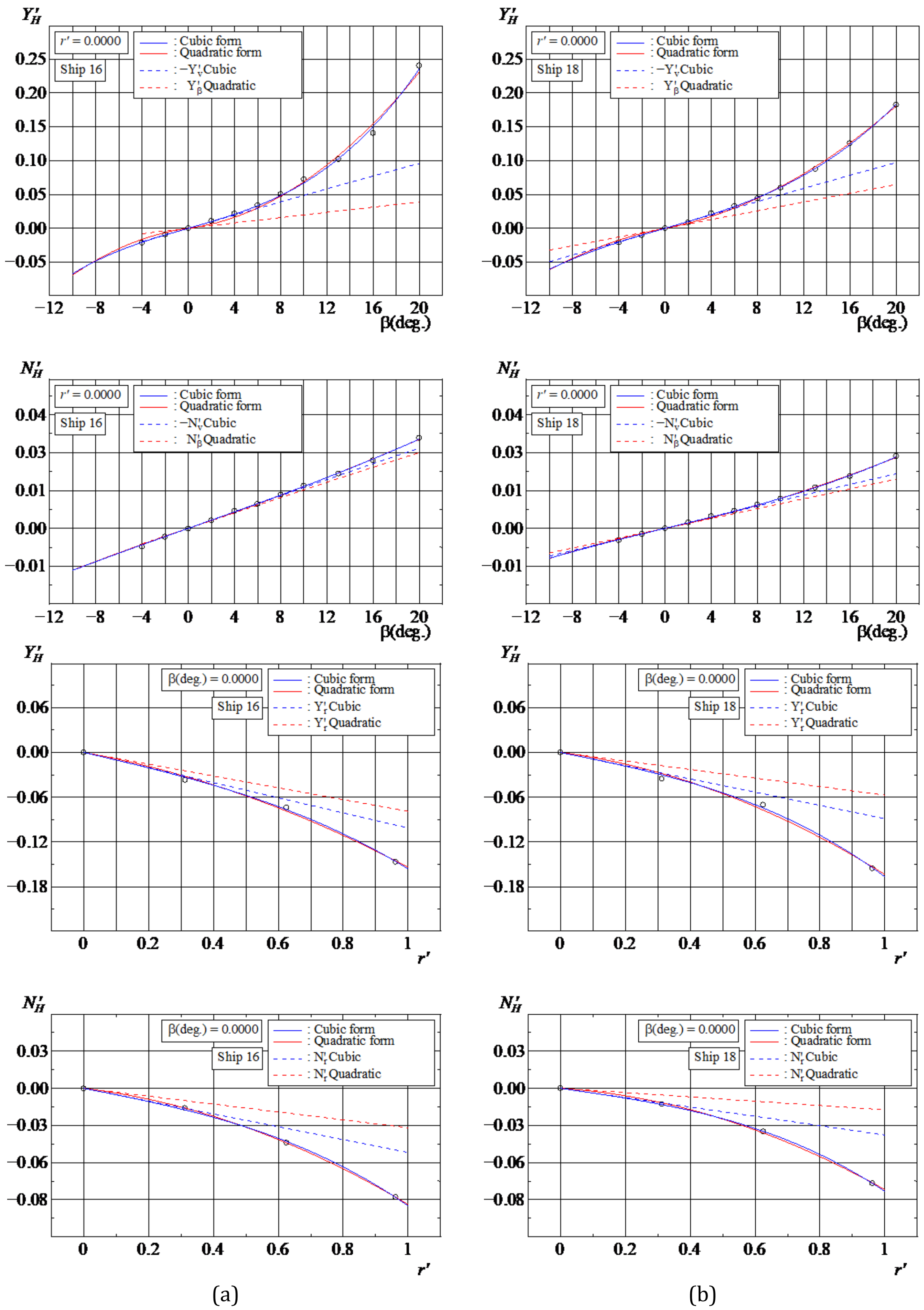

Figure 14 Category 3 - The Y_H' and N_H' curves of Ship F were modelled for both loading conditions (a) Fully loaded condition and (b) Ballast condition

The discrepancy between the cubic and quadratic models results can be attributed to differences in the values of linear hydrodynamic derivatives. By examining the course stability index values in Equation (12), it is evident that ships with different signs of *Δ* have varying linear derivatives between the two models. For instance, Ship No. 17 exhibits a different sign in the *Δ*. Figure 15 shows that both models have different absolute values for the 1st and 2nd terms of the Δ for all ships. In the quadratic model, $Y'_\beta N'_r$ has a smaller absolute value compared to $N'_\beta\{Y'_r - (m' + m'_x)\}$, whereas the cubic model shows the opposite. This discrepancy is due to the distinct characteristics of the two functions. In general, when the nonlinearity of the data is low, a quadratic function tends to have smaller linear derivatives compared to a cubic model. This is supported by the data in Figure 15, where the absolute values of the Δ terms in the quadratic model are consistently smaller than those in the cubic model.

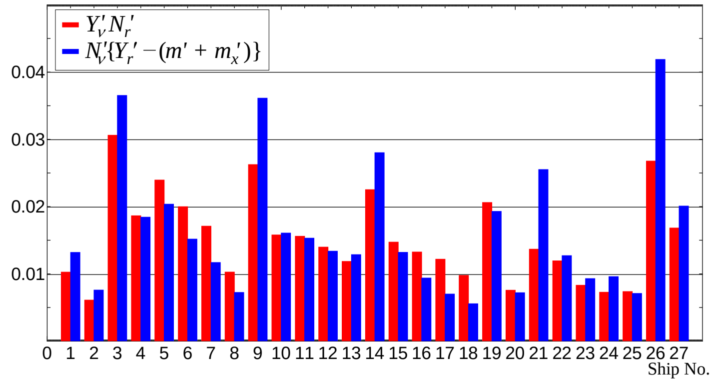

(a)

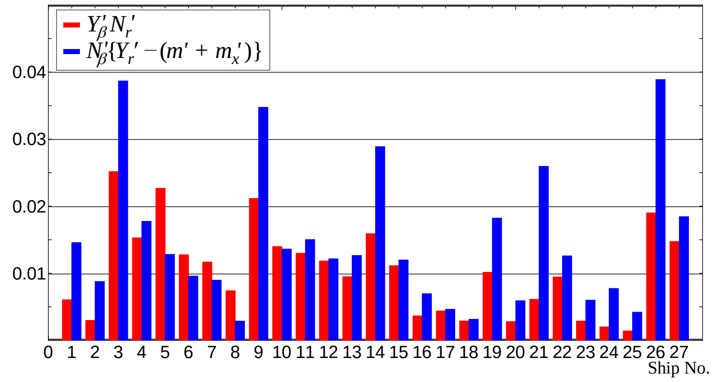

(b)

Figure 15 Comparison of the linear derivatives absolute value (a) cubic model and (b) quadratic model

Moreover, most ships with fully loaded and ballast conditions, including Esso Osaka Ship C, Ship, Ship E, and Ship I, show pretty much all the different signs of Δ in both the cubic and quadratic models. However, there are exceptions, such as Ship F and Ship G, where both ships show distinct signs of Δ between the two models in all loading conditions.

Both models in Category 1 consistently yield the same results regardless of whether $Y'_\beta N'_r$ is greater than $N'_\beta\{Y'_r - (m' + m'_x)\}$ or vice versa. However, there is a difference in results in categories 2 and 3. The value of $Y'_\beta N'_r$ is greater than $N'_\beta\{Y'_r - (m' + m'_x)\}$ only for the quadratic model. This indicates the importance of considering the discrepancies in linear hydrodynamic derivatives between both mathematical models when assessing the course stability of a ship in ballast conditions.

Next, we compare ships from Category 1 with ships from Category 2 or 3 for all loading conditions. Ship No. 1 and Ship No. 2 from Category 1 (SR108) are compared with Ship No. 16 and Ship No. 18 from Category 3 (Ship F). These ships were chosen because they are both container carriers, but they have different Δ tendencies that need to be investigated.

Figure 16 evaluates the differences in values between the first and second terms without taking into account the negative signs in Equation (12) between Ship No. 1 and Ship

No. 16. In Ship No. 1, both mathematic models show that the absolute value of $Y'_\beta N'_r$ is smaller than $N'_\beta\{Y'_r - (m' + m'_x)\}$. However, the cubic model for Ship No. 16 shows a different outcome. This discrepancy in absolute values is attributed to the limited experimental data and mathematical differences between the two models, as previously discussed.

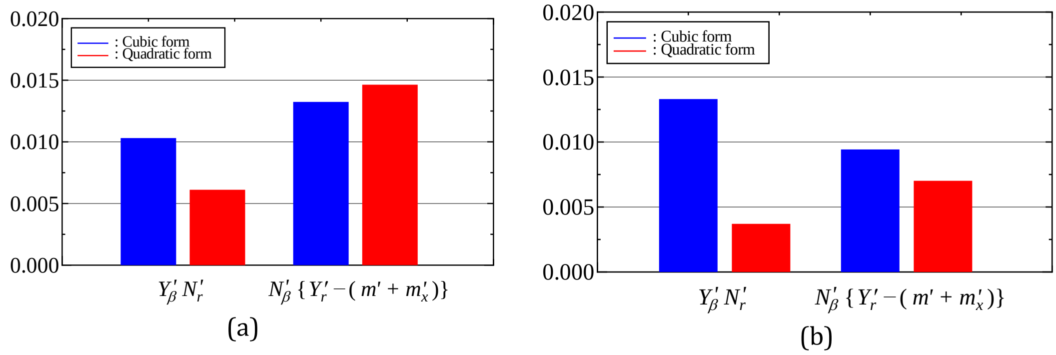

Figure 16 $Y'_\beta N'_r$ and $N'_\beta\{Y'_r - (m' + m'_x)\}$ Comparison (a) ship no. 1 and (b) ship no 16

It has been verified that there are variations in the results obtained from the cubic and quadratic models when measuring hydrodynamic forces at different drift angles. To further explore these differences in calculating Δ, the locations where yaw and sway damping force are applied to all ships are analyzed. It is observed that the quadratic model generally yields a lower value compared to the cubic model.

4. Conclusions

Manoeuvring motion and two mathematical models for lateral force and yawing moment using cubic and quadratic polynomials have been discussed. The cubic model is more accurate for hydrodynamic forces measured over a large range of motion, while the quadratic model may be more accurate for smaller ranges. It is important to consider these differences when using the cubic model for turning tests and CMT on a small range of β and r'. On the other hand, the comparison of Δ results between the cubic and quadratic models are examined. The discrepancy in Δ is attributed to the varying linear hydrodynamic derivatives in the two models. The presence of measured hydrodynamic forces across a wide range of drift angles leads to divergent outcomes between both mathematical models. This highlights the importance of carefully considering the differences in linear hydrodynamic derivatives from the cubic and quadratic models when assessing the course stability index under ballast conditions.

References

Ayub, F. A., Furukawa, Y., Ibaragi, H. 2021. Sensitivity Analysis of Hydrodynamic Derivatives for Lateral Force and Yawing Moment. *In:* 31st International Ocean and Polar Engineering Conference (ISOPE), Rhodes, Greece, p. 4175

Berge, S.P., Fossen, T.I., 2000. On the Properties of the Nonlinear Ship Equations of Motion. *Mathematical and Computer Modelling of Dynamical Systems,* Volume 6(4), pp. 365–381

Dash, A.K., Nagarajan, V., Sha, O.P. 2015, Uncertainty Assessment for Ship Manoeuvring Mathematical Model, *International Ship Building Progress*, Volume 61, pp. 129–161

Degrieck, A., Uyttersprot, B., Sutulo, S., Guedes Soares, C., Wim Van Hoydonck, Vantorre M., Lataire E., 2021. Hydrodynamic Ship–Ship and Ship–Bank Interaction: A Comparative Numerical Study, *Ocean Engineering,* Volume 230, p. 108970

Fedyaevsky, K.K., Sobolev, G.V., 1963a. *Control and Stability in Ship Design*. Leningrad: State Union Ship Building Publishing House

Fedyaevsky, K.K., Sobolev, G.V., 1963b. *The Handling Qualities of Ships*. Leningrad: Sudpromgiz,

Fossen, T.I., 2011. Handbook of Marine Craft Hydrodynamics and Motion Control. Chichester, UK: John Wiley & Sons, Ltd.

Gavrilin, S., Steen, S., 2016, An Alternative Approach to Validation of Ship Manoevring Models*. In:* ASME 2016 35th International Conference on Ocean, Offshore and Arctic Engineering, p. 54276

Hasanvand, A., Hajivand, A., 2019. Investigating the Effect of Rudder Profile on 6DOF Ship Turning Performance. *Applied Ocean Research,* Volume 92, p. 101918

Inoue, S., 1978. The Hydrodynamic Derivatives on Ship Manoeuvrability in Even Keel Conditions*. In:* Proceeding of 15th International Towing Tank Conference (ITTC)

International Maritime Organization (IMO), 2002. Standards for Ship Manoeuvrability, Annex 6 Resolution MSC.137(76). International Maritime Organization

Islam, H., Soares, C., 2018. Estimation of Hydrodynamic Derivatives of a Container Ship Using PMM Simulation in OpenFOAM. *Ocean Engineering*, Volume 164, pp. 414–425

ITTC Manoeuvring Committee, 2008. Report of the Manoeuvring Committee. *In:* Proceeding of 25th International Towing Tank Conference (ITTC), Fukuoka, pp. 143–208

ITTC Manoeuvring Committee, 2011. Report of the Manoeuvring Committee*. In:* Proceeding of 26th International Towing Tank Conference (ITTC), Rio de Janeiro, pp. 123–181

ITTC Manoeuvring Committee, 2017. *Recommended Procedure and Guidelines: Uncertainty Analysis for Manoeuvring Predictions based on Captive Manoeuvring Tests*, 7.5-02-06-04, Revision 2, p. 33

Kang, D., Hasegawa, K., 2007. Prediction Method of Hydrodynamic Forces Acting on The Hull of a Blunt-Body Ship in The Even Keel Condition. *Journal of Marine Science and Technology,* Volume 12, pp. 1–14

Karasuno, K., Okano, S., Miyoshi, J., Maekawa, K., 2003. Predictions of Ship's Hull Hydrodynamic Forces and Manoeuvring Motions at Slow Speed Based on a Component type Mathematical Model. *In:* Proceeding MARSIM'03, Kanazawa, pp. 25–28

Kijima, K., Katsuno, T., Nakiri, Y., Furukawa, Y., 1990. On the Manoeuvring Performance of a Ship with the Parameter of Loading Condition, *Journal of The Society of Naval Architects of Japan*, Volume 168, pp. 141–148

Liu, Y., Zou, Z., Zou, L., Li, B., 2018. URANS Simulation of Dynamic Captive Model Tests Considering the Effect of Ship Attitude Change. 13th International Conference on Hydrodynamics, Incheon, Korea, pp. 291–300

Luo, W., Guedes Soares, C., Zou, Z., 2016. Parameter Identification of Ship Maneuvering Model Based on Support Vector Machines and Particle Swarm Optimization. *Journal of Offshore Mechanics and Arctic Engineering,* Volume 138(3), p. 031101

Viallon, M., Sutulo, S., Soares, C.G., 2012. On the Order of Polynomial Regression Models for Manoeuvring Forces. *In:* IFAC Proceedings Volumes, Volume 45(27), pp. 13–18

Oltmann, P., Sharma, S.D., 1984. Simulation Of Combined Engine and Rudder Maneuvers Using an Improved Model Of Hull-Propeller-Rudder Interactions. *In:* Proceedings of 15th ONR Symposium on Naval Hydrodynamics. Hamburg, Washington, D.C., pp. 83–108

Sawada, R., Hirata, K., Kitagawa, Y., Saito, E., Ueno, M., Tanizawa, K., Fukuto, J., 2021. Path Following Algorithm Application to Automatic Berthing Control. *Journal of Marine Science and Technology,* Volume 26, pp. 541–554

Shenoi, R., Krishnankutty, P., Selvam, R.P., 2015. Sensitivity Study of Hydrodynamic Derivative Variations on the Maneuverability Prediction of a Container Ship. *In:* International Conference on Offshore Mechanics and Arctic Engineering, Volume 56550, p. V007T06A008

Shouji, K., Ohtsu, K., 1992, A Study of Optimization of Ship Manoeuvring by Optimal Control Theory (1st Report), *Journal of the Society of Naval Architects of Japan*, Volume 172, pp. 365–373

Tao, R., Sichen, T., Yun, Y., Huan, Z., 2021. Research and Application on Mathematical Model of Ship Manoeuvring Motion under Shallow Water Effect. IOP Conference Series: Earth and Environmental Science, Volume 643(1), p. 012127

Toxopeus, S., 2011a. *Practical Application of Viscous-Flow Calculation for the Simulation of Manoeuvring Ships.* Delft University of Technology

Toxopeus, S., 2011b. Viscous-Flow Calculations for KVLCC2 in Deep and Shallow Water. *In:* International Conference on Computational Methods in Marine Engineering, Lisbon, Portugal, pp. 151–169

Toxopeus, S.L., 2007. Deriving Mathematical Manoeuvring Models for Bare Hull Ships Using Viscous-Flow Calculations. *In:* Marine International Conference on Computational Methods in Marine Engineering, Volume 14(1), pp. 0948–4280

Wang, X.G., Zou, Z.J., Xu, F., Ren, R.Y., 2014, Sensitivity Analysis and Parametric Identification for Ship Manoeuvring in 4 Degrees of Freedom. *Journal of Marine Science and Technology*, Volume 19, pp. 394–405

Woodward, M., 2013. Propagation of Experimental Uncertainty from Force Measurements into Manoeuvring Derivatives. *In:* 3rd International Conference on Advanced Model Measurement Technology, Gdansk, Poland

Woodward, M.D., 2014. Evaluation of Inter-Facility Uncertainty for Ship Manoeuvring Performance Prediction, *Ocean Engineering*, Volume 88, pp. 598–606.

Yasukawa, H., Sakuno, R., 2020. Application of the MMG Method for The Prediction of Steady Sailing Condition and Course Stability of A Ship Under External Disturbances. *Journal of Marine Science and Technology,* Volume 25, pp. 196–220

Yasukawa, H., Yoshimura, Y., 2015. Introduction of MMG Standard Method for Ship Manoeuvring Predictions, *Japan Marine Science and Technology*, Volume 20, pp. 37–52

Yoshimura, Y., 1988. Mathematical Model for Manoeuvring Ship Motion In Shallow Water (2nd report) - Mathematical Model At Slow Forward Speed. *Journal of Kansai Society of Naval Architects*, Volume 210, pp. 77–84

Yoshimura, Y., 2001 Investigation Into The Yaq-Checking Ability In Ship Manoeuvrability Standard. *In:* Proceedings of Prediction of Ship Manoeuvring Performance, Tokyo, JAPAN

Yoshimura, Y., Nakao, I., Ishibashi, A., 2009. Unified Mathematical Model for Ocean and Harbour Manoeuvring. *In:* Proceedings of MARSIM 2009, pp. 116–124

Yang, Y., Chillcce, G., El Moctar, O., 2023. Mathematical Modeling of Shallow Water Effects on Ship Maneuvering, *Applied Ocean Research,* Volume 136, p. 103573

Yang, Y., el Moctar, O., 2024. A Mathematical Model for Ships Maneuvering In Deep And Shallow Waters. *Ocean Engineering,* Volume 295, p. 116927

Yukawa, K., Kijima, K., 1998, An Estimation of Course Stability at Initial Design Stage. *Journal of the Society of Naval Architects of Japan,* Volume 184, pp. 63–70

Zhang, S., Qing W., Jialun L., Yangying H., Shijie L., 2023. State-of-the-Art Review and Future Perspectives on Maneuvering Modeling for Automatic Ship Berthing. *Journal of Marine Science and Engineering*, Volume 11(9), p. 1824